

We are IntechOpen, the world's leading publisher of Open Access books Built by scientists, for scientists

6,300

Open access books available

171,000

International authors and editors

190M

Downloads

Our authors are among the

154

Countries delivered to

TOP 1%

most cited scientists

12.2%

Contributors from top 500 universities



WEB OF SCIENCE™

Selection of our books indexed in the Book Citation Index
in Web of Science™ Core Collection (BKCI)

Interested in publishing with us?
Contact book.department@intechopen.com

Numbers displayed above are based on latest data collected.
For more information visit www.intechopen.com



Chapter

A Review of Particle Removal Due to Thermophoretic Deposition

Yonggang Zhou, Mingzhou Yu and Zhandong Shi

Abstract

Thermophoretic deposition is an important technique for particle removal. The thermophoretic force of the particles under an appropriate temperature gradient can achieve a good particle removal effect. At present, there have been many studies on the deposition mechanism of ultrafine particles under the action of thermophoresis. In this chapter, the development history and current research status of the research on the thermophoretic deposition effect of ultrafine particles are summarized, and the future direction of thermophoretic deposition is proposed.

Keywords: ultrafine particle, deposition, thermophoresis, mathematical model

1. Introduction

Fine particles play an important role in environmental gas pollution, which are smaller than coarse particles. These particles are main driver of urban haze formation, and also the main component of tobacco aerosol and kitchen fumes. They have an aerodynamic diameter of $2.5\mu\text{m}$ or less (PM_{2.5}). The fine particles which are smaller than $0.1\mu\text{m}$ are referred to as ultrafine particles (PM_{0.1}). These particles can often be suspended in the air and enter the respiratory tract of the human body along with the human body's respiration. Since the surface of fine particle is usually attached to harmful substances such as bacteria and heavy metals, it is easy to cause respiratory diseases and endanger human health after entering the human body [1]. Ebenstein et al. [2] found that combined atmospheric pollution has a significant impact on life expectancy and mortality from cardiopulmonary diseases. For every $100\mu\text{g}/\text{m}^3$ increase in the concentration of air pollutants, the life expectancy of people under 5 years old is reduced by 1.5 years, and the life expectancy of people over 5 years old is reduced by 2.3 years. Cardiopulmonary diseases cause an increase of 79 deaths per 100,000 people. In 2016, a Polish cohort study of healthy school-age children aged 13–14 years found that for every quartile unit increase in PM₁ concentration, forced vital capacity (FVC) and peak expiratory flow (PEF) decreased by 1.0 and 4.4% respectively [3]. With the continuous development of manufacturing technology, in some electronic equipment and industrial products, the pollution caused by particle deposition affects both the yield and the use process. Some fine particles, after absorbing moisture in the air, will deposit on the surface of the equipment and form an electrolytic layer, which can have a corrosive effect on many metals. If the electrolyte

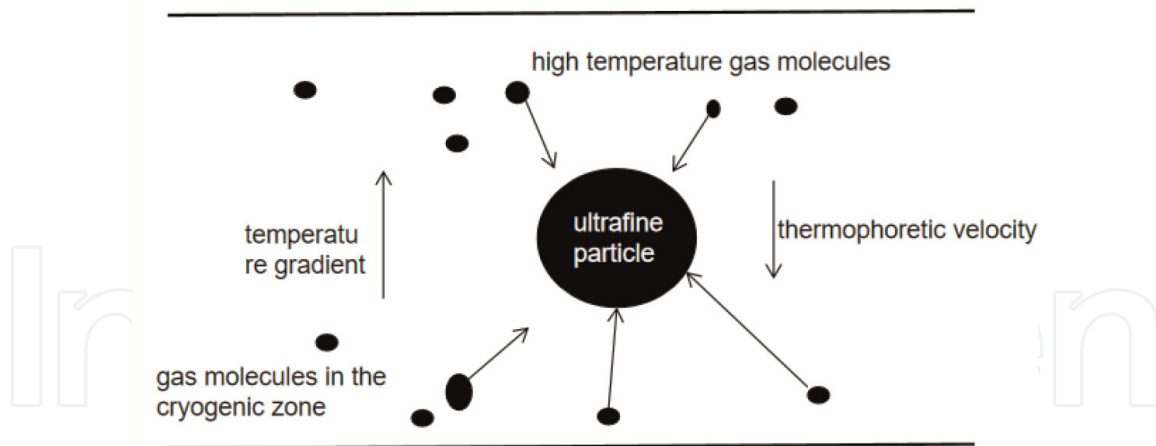


Figure 1.
Basic schematic diagram of thermophoresis.

penetrates into the protective layer of the wire to form corrosion points, an arc may be generated between the wire and the conductor to burn out the components.

The thermophoretic effect plays a very important role in the deposition of fine particles, so it is necessary to study the thermophoretic deposition of fine particles. In 2012, Ström and Sasic [4] studied the improvement of particle deposition efficiency in diesel or gasoline aftertreatment systems by thermophoresis. Their results show that for a standard monolithic channel with a gas-to-wall temperature difference of 200 K, deposition efficiencies of around 15% may be possible for all particle sizes. Some scholars have also applied it to the utilization of water resources. Dhanraj and Harishb et al. [5] designed a device to extract water from the air by thermophoresis and condensation. In the microgravity environment, thermophoresis plays a more critical role, and thermophoresis may be an important way of fine particle transfer. In the microgravity environment in space, it is of great significance to consider the influence of the thermophoresis mechanism in the aerospace field.

Although thermophoresis was discovered as early as the eighteenth century, its fundamental physical process was not proposed by Maxwell until 1879. In an area with a certain temperature difference, the gas molecules in the hot and cold areas continue to hit the particles. Since the gas molecules in the hot area have a large momentum, after hitting the particles, the macroscopically shows that the particles are subjected to force from the hot area to the particle. The phenomenon of movement of the cold zone, this force is the thermophoretic force [6]. Based on the formula of thermophoretic force, scientists derived formulas of thermophoretic deposition rate. In this chapter, the studies on both thermophoretic force and deposition rate due to thermophoresis are reviewed (**Figure 1**).

2. Thermophoretic deposition

In the temperature field with a certain temperature difference, the gas molecules and particles in the hot zone move to the hot zone again due to the reaction force after colliding with the particles. This phenomenon is called thermal glide. Maxwell (1879) and Reynolds (1880) analyzed the relationship between the flow field and the temperature field theoretically and experimentally [7] and determined the phenomenon of thermal slip. Maxwell proposed that the slip velocity of the gas is [8]:

$$\vec{v}_c = -\frac{3}{4}\nu\nabla\ln T \quad (1)$$

where ν is the gas kinematic viscosity, T is the gas temperature.

2.1 Models of thermophoretic force

According to Maxwell's description and slip boundary conditions, Epstein selected spherical particles in the gas as the object, and he solved the Navier-Stokes equation with the boundary conditions of the temperature gradient field considering the heat transfer heat balance. Finally, he first obtained the formula of thermophoretic force on the particles in the continuum region [9]:

$$F_T = \frac{9\pi\mu\nu d_p \nabla T}{2T_o} \left(\frac{k_g}{k_p + 2k_g} \right) \quad (2)$$

where μ is fluid viscosity, d_p is particle diameter, k_g is fluid thermal conductivity coefficient, k_p is particle thermal conductivity coefficient, T_o is the average temperature of fluid near particle. Epstein's conclusion is in good agreement with the experimental results when k_p is low and the thermal conductivity coefficient of the particles is low, but the theoretical value of this result is far from the experimental results when the thermal conductivity coefficient of the particles is high (L. [10]). Derjaguin and Storozhilova et al. [11]. pointed out that if high thermal conductivity particles such as sodium chloride are used, the actual thermophoretic force is two orders of magnitude higher than the theoretical [11].

In 1958, Waldmann [12] deduced the expression of the thermophoretic force of particles in the free molecular region in a single atomic gas based on the principle of molecular dynamics and the rigid body collision model between gas molecules and particles:

$$F_{th} = -\frac{16\sqrt{\pi}}{15} \frac{R^2 k_g}{\sqrt{\frac{2k_B T}{m_g}}} \nabla T \quad (3)$$

where k_B is Boltzmann constant, m_g is gas molecular mass, R is particle radius.

In 1962, based on Epstein's theory, Brock deduced the expressions of particle thermophoretic velocity and thermophoretic force applicable to the continuum region to the free-molecular region by applying the first-order slip-flow boundary conditions [13, 14]:

$$U_T = -\frac{2\nu C_s \left(\frac{k_g}{k_p} + 2C_t \frac{\lambda}{d_p} \right) \frac{(\nabla T)_x}{T_o}}{\left(1 + 4C_m \frac{\lambda}{d_p} \right) \left(1 + 2\frac{k_g}{k_p} + 4C_t \frac{\lambda}{d_p} \right)} \quad (4)$$

$$F_T = -\frac{12\pi\mu\nu R C_s \left(\frac{k_g}{k_p} + C_t \frac{\lambda}{R} \right) \frac{(\nabla T)_x}{T_o}}{\left(1 + 3C_m \frac{\lambda}{R} \right) \left(1 + 2\frac{k_g}{k_p} + 2C_t \frac{\lambda}{R} \right)} \quad (5)$$

where λ is the mean free path of gas molecules, C_s (0.75), C_m (1.14), and C_t are dimensionless constants, which are thermal slip coefficient, viscous slip coefficient, and temperature jump coefficient, respectively. Although the result of Brock still differs from the experimental value when the particles have a high thermal conductivity coefficient, it is already much smaller than Epstein's error.

Derjaguin [15] pointed out that Brock's assumption that the gas molecules always have the same velocity distribution before hitting the particle interface is inaccurate whose velocity distributions in the Knudsen layer vary with distance from the wall in the presence of a tangential temperature gradient. Through experiments, it is pointed out that its velocity formula (Eq. 4) does not conform to the experimental results at medium and large particle sizes (0.3–0.6 μm).

In 1980, Talbot [10] used laser-Doppler velocimeter (LDV) to measure the thickness of the particle void region produced by the particle velocity distribution in the laminar boundary layer at the heated wall under the action of thermophoretic force. According to the experimental results and the BGK model in the particles, it is found that the reason for the large error of the Brock thermophoretic force formula (Eq. 4) is the problem of the thermal slip coefficient C_s , and the value of it is corrected to 1.17. Talbot also proposed the expression of the thermophoresis coefficient k_{th} . Although the revised thermophoretic force expression is still not perfect, it has been widely used.

Cha, McCoy [16] and Wood [17] deduced a thermophoretic calculation model with good applicability in a wide range of Knudsen numbers. Although the theoretical calculation results and the experimental data reported by other scholars at that time have small numerical errors, they are in good agreement with the overall trend. After correcting the correlation coefficient, the calculated result is in good agreement with the result of Talbot's formula when $k_n < 3$. The corrected expression is:

$$F_{th} = 1.15 \frac{Kn}{4\sqrt{2}\alpha \left(1 + \frac{\pi_1}{2} Kn\right)} \cdot \left[1 - \exp\left(-\frac{\alpha}{Kn}\right)\right] \cdot \left(\frac{4}{3\pi} \phi \pi_1 Kn\right)^{0.5} \frac{k_B}{d_m^2} \nabla T d_p^2 \quad (6)$$

$$\alpha = 0.22 \left[\frac{\frac{\pi}{6} \phi}{\left(1 + \frac{\pi_1}{2} Kn\right)} \right]^{\frac{1}{2}} \quad (7)$$

$$\pi_1 = \frac{0.18 \left(\frac{36}{\pi}\right)}{\left[\frac{(2 - S_n + S_t)4}{\pi} + S_n \right]} \quad (8)$$

where d_p is the equivalent diameter of the channel, C_v is the constant volume-specific heat capacity, C_m is the conventional momentum adjustment coefficient, and C_t is the tangential momentum adjustment coefficient.

In 2003, Li and Wang [18, 19] deduced the theoretical calculation formula of the thermophoretic force on nanoparticles in the free molecular region based on the non-rigid collision model:

$$F_{T,Li} = -\frac{8}{3} \sqrt{\frac{2\pi m_r}{k_B T}} \kappa R^2 \nabla T \left(\frac{6}{5} \Omega^{(1,2)*} - \Omega^{(1,1)*} \right) \quad (9)$$

In the formula, m_r is the mass of particles, κ is thermal conductivity of gases, $m_r = m_g m_p / (m_g + m_p)$, is the reduced mass of gas molecules and particles; $\Omega^{(1,1)*}$ and $\Omega^{(1,2)*}$ are the dimensionless collision integral, for rigid body collision,

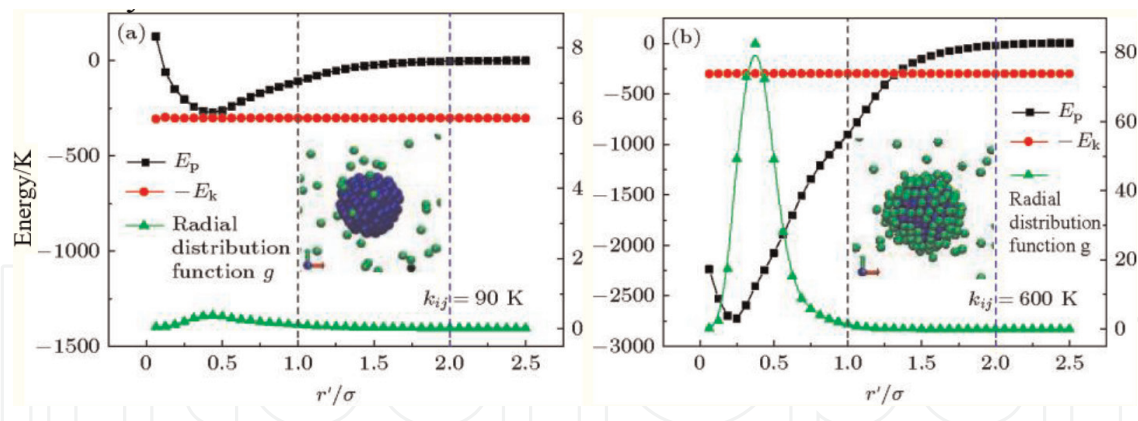


Figure 2. The potential energy E_p , kinetic energy E_k and density function g on the surface of nanoparticles Cui et al. [20].

$\Omega^{(1,1)*} = \Omega^{(1,2)*} = 1$. Eq. (3) is a special case of Eq. (9). But Li and Wang's theoretical model has not been experimentally demonstrated. Due to the insufficiency of nano-scale particle measurement technology, it is often difficult to study the corresponding thermophoresis phenomenon in experiments. Cui et al. [20] used molecular dynamics simulation to verify the theoretical calculation model of Waldmann [12] and Li [18, 19] found that when the particle size was reduced to the nanometer scale, Waldmann's calculation model is no longer applicable due to the enhancement of the non-rigid collision effect, and the theoretical model established by Li and Wang after considering the non-rigid collision effect is closer to the molecular dynamics simulation results. At high gas-solid bonding strength, gas molecules are easily adsorbed on nanoparticles, which changes the true particle size of the particles (Figure 2), resulting in a certain error in the correction formulas of Li and Wang [18, 19]. Cui et al. [20] corrected the particle size error and the results were basically consistent with the simulated values.

In terms of thermophoresis measurement technology, it is mainly divided into particle group measurement and single particle measurement. In the measurement using the particle group, the gas stream with particles enters a vacuum chamber with a temperature gradient in the vertical direction. Calculations are often inaccurate. Particle size can be determined when individual particles are measured, so it tends to be more precise. Li and Davis [21] used electrodynamic balance (EDB) to measure individual particles and compared with previous theories and obtained better data result (Figure 3).

2.2 Models of thermophoretic deposition efficiency

In the calculation of the deposition efficiency of thermophoresis, many scholars have established their expressions. Since the theoretical calculation models of various scholars under laminar flow conditions can be well in line with the experimental or simulated values, the calculation model of thermophoretic deposition efficiency under turbulent flow conditions is mainly introduced here.

In 1969 Byers and Calver [22] measured the influence of flow parameters and particle collector size on deposition efficiency and established the thermophoretic deposition efficiency expression:

$$\eta_L = 1 - \exp\left(-\frac{\rho C_p f \text{Re}_D K_{th} v (T_e - T_w)}{4Dh \bar{T}} \left(1 - \exp\left(\frac{-4hL}{u_m \rho C_p D}\right)\right)\right) \quad (10)$$

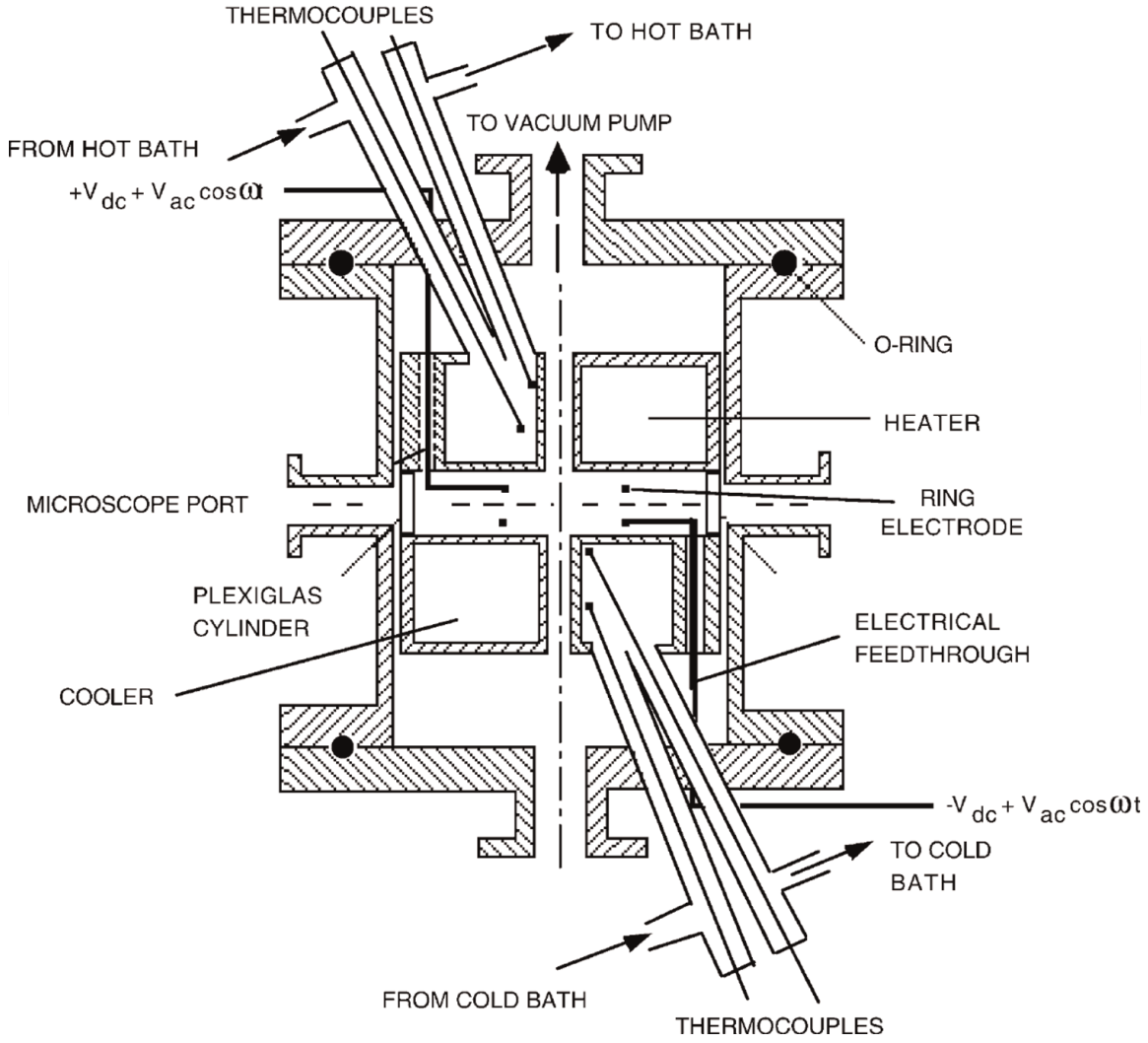


Figure 3. A cross-section of the electrodynamic balance and vacuum chamber used by Li and Davis for thermophoretic force measurements [21].

where c_p is the specific heat capacity of the gas at constant pressure, T_e and T_w are the fluid inlet and tube wall temperatures respectively, K_{th} is thermophoretic coefficient, \bar{T} is the average temperature, h is the convective heat transfer coefficient, L is the tube length, D is the tube diameter, ρ is the gas density, f is the coefficient of friction, u is the average radial velocity.

In 1974, Nishio experimentally determined the deposition of aerosols on the temperature gradient along the length of the heat exchanger tube wall,

$$\eta_L = 1 - \exp\left(-\frac{\rho C_p K_{th} v (T_e - T_w)}{k_g \bar{T}} \left(1 - \exp\left(\frac{-4hL}{u_m \rho C_p D}\right)\right)\right) \quad (11)$$

Batchelor and Shen [23] used the similarity method to analyze the deposition rate as the pipe length by thermophoretic effects in flow over plates, cylinders, and rotating bodies,

$$\eta_L = \text{Pr} K_{th} \left(\frac{T_e - T_w}{T_e}\right) \left(1 + (1 - \text{Pr} K_{th}) \left(\frac{T_e - T_w}{T_e}\right)\right) \quad (12)$$

Where is Prandtl number of air.

In 1998, Romay et al. [24] conducted experiments in turbulent pipelines, respectively measured the influence of inlet flow velocity, flow rate, particle size, and inlet fluid temperature on the deposition efficiency of the pipeline, and compared them with the existing theoretical model Eqs. (10) and (11) of deposition efficiency at that time. For comparison, an expression for the deposition efficiency of thermophoresis in a turbulent tube is derived:

$$\eta_L = 1 - \left[\frac{T_w + (T_e - T_w) \exp\left(-\frac{\pi D h L}{\rho Q C_p}\right)}{T_e} \right]^{Pr K_{th}} \quad (13)$$

Q is the volume flow (Figure 4).

The above one-dimensional expressions are all derived under specific assumptions, and cannot be well applied to general engineering specifications. In 2005, Housiadas and Drossinos [25] developed a two-dimensional model including radial section effects after establishing the one-dimensional long-tube deposition efficiency expression suitable for laminar and turbulent flow and carried out extensive verification. Its one-dimensional expression is:

$$\eta_L = 1 - \left(\frac{\theta^*}{1 + \theta^*} \right)^{Pr K_{th}} = 1 - \left(\frac{T_w}{T_e} \right)^{Pr K_{th}} \quad (14)$$

There are many studies on the calculation of key parameters under the thermophoretic effect. Because the preconditions selected by each scholar are different, the establishment of the final expression is also different. Early studies on

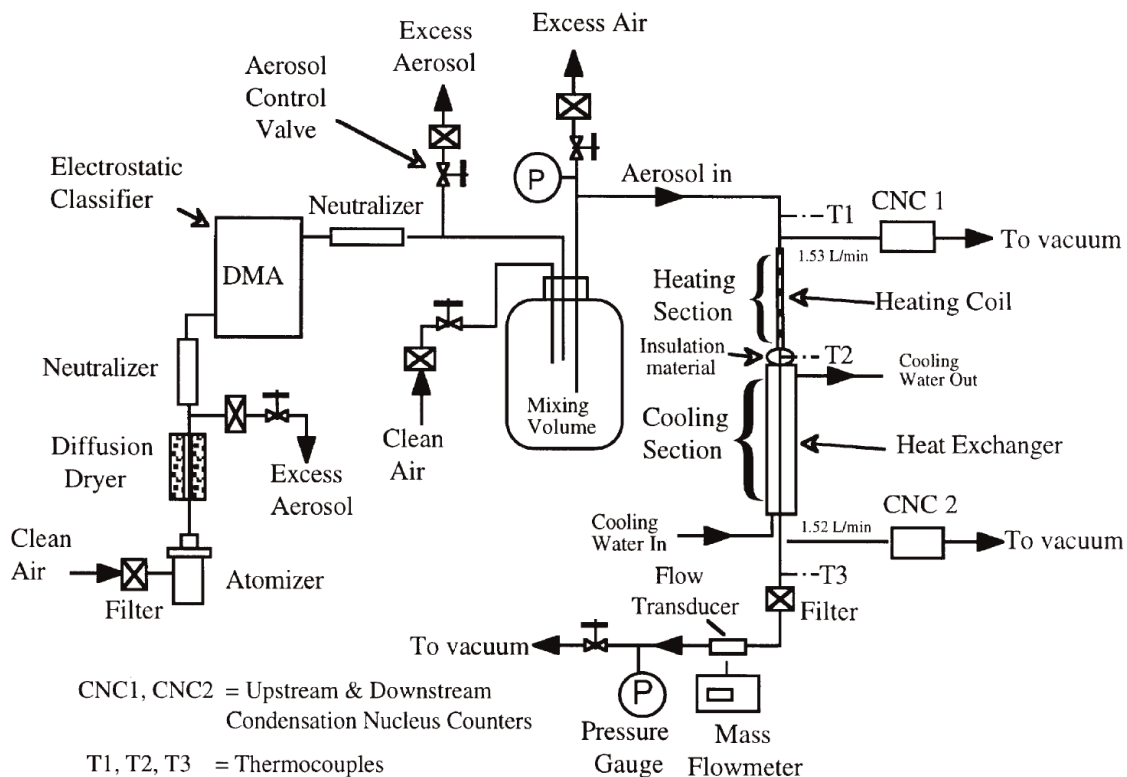


Figure 4. Schematic diagram of the experimental apparatus by Romay et al. [24].

thermophoretic deposition effects mostly focused on the mechanism. In recent years, with the maturity of numerical simulation and particle detection technologies, more scholars have begun to consider the performance of thermophoretic deposition in different scenarios. The development direction is gradually diversified.

3. Current status of particle thermophoretic deposition

At present, there are three main ways to study the thermophoretic effect: theoretical research, numerical simulation, and experimental research. Researchers deduce new empirical expressions based on existing theories through numerical simulations or experiments under selected specific experimental conditions. The force characteristics and motion trajectory of the particles are analyzed, and the particle motion model of the thermophoresis effect under different conditions is established. The main work is divided into three categories. One is the influence of particle shape on thermophoretic effect, the other is the study of thermophoretic deposition effect of particles in pipes or small spaces, and the changes in particle concentration distribution or deposition law caused by thermophoretic effect in indoor and outdoor temperature fields. The following is an overview of the results of the main research groups currently working on both types of work.

3.1 Research on thermophoretic deposition in pipes and tiny spaces

Thermophoretic effects in pipes or tiny spaces are a hot topic in current thermophoretic research. The researchers selected specific flow field conditions and pipeline structures and established corresponding particle motion models based on existing theories through experiments and numerical simulations. The research team of Lin and Tsai of National Chiao Tung University used the critical trajectory method to study the effect of developing flow in a circular tube on the deposition efficiency of thermophoretic particles [26]. Through theoretical and numerical analysis, a dimensionless equation for calculating thermophoretic deposition efficiency under laminar flow conditions is established. The research results show that the inlet section where the velocity and temperature are both developing is more conducive to the formation of thermophoretic sedimentation of particles due to the existence of a relatively large temperature gradient, resulting in higher thermophoretic deposition efficiency. They determined the effect of particle diffusion and particle electrostatic charge induced deposition on thermophoretic deposition efficiency in laminar and turbulent tubes [27] (**Figure 5**). It is found that the deposition efficiency caused by the electrostatic charge of particles is comparable to the thermophoretic deposition efficiency when the thermophoretic efficiency is usually lower than 10% in their experiments (**Figure 6**), so this effect should be excluded when calculating the thermophoretic deposition efficiency to obtain accurate experimental data. Even for particles in Boltzmann charge balance, the deposition efficiency of the particle electrostatic charge has a considerable effect compared to the thermophoretic deposition efficiency. In addition, Tsai et al. also studied the inhibition process of particle thermophoretic deposition through the tube wall when the tube wall temperature exceeds the gas temperature in a circular tube [28]. The particle transport equations of convection, diffusion, and thermophoresis were numerically solved, and the particle concentration distribution and deposition laws were obtained. The results show that for all particle sizes, the particle deposition rate decreases with increasing tube wall

temperature and gas flow rate. When the tube wall is heated to a certain temperature slightly above the gas temperature, particle deposition is completely suppressed. And given dimensionless deposition parameters, an empirical expression is established to predict the dimensionless temperature difference required for zero deposition in laminar flow tubes (Figures 5 and 6).

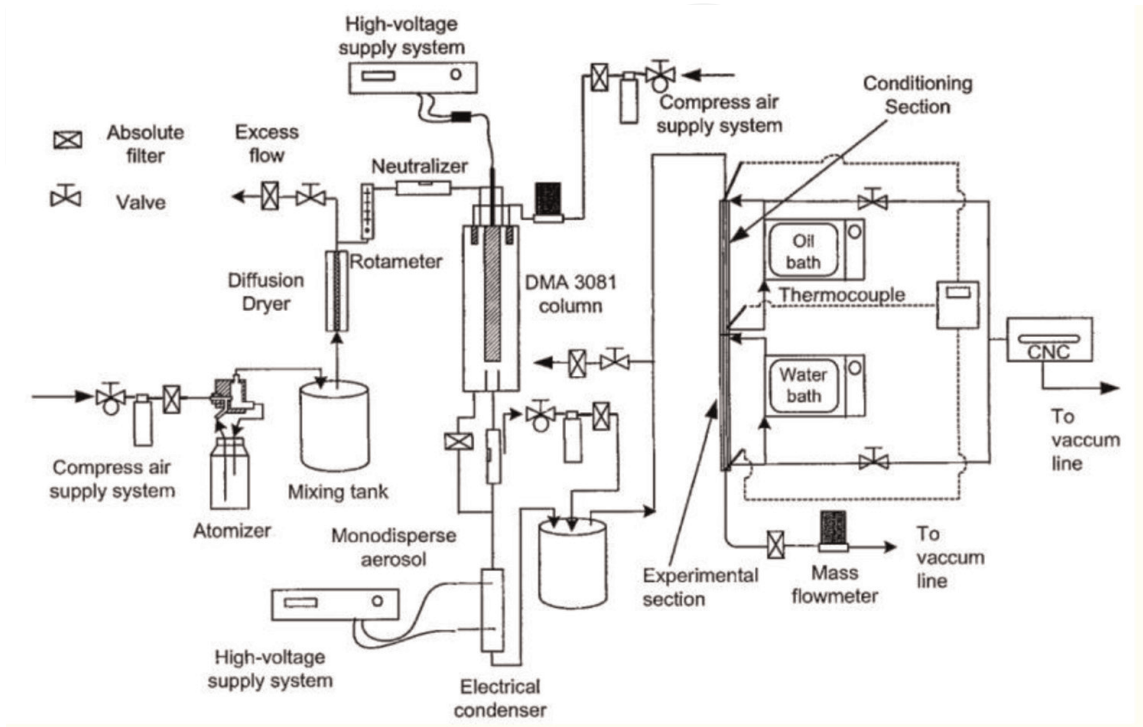


Figure 5. Schematic diagram of the experimental apparatus by Lin and Tsai [27].

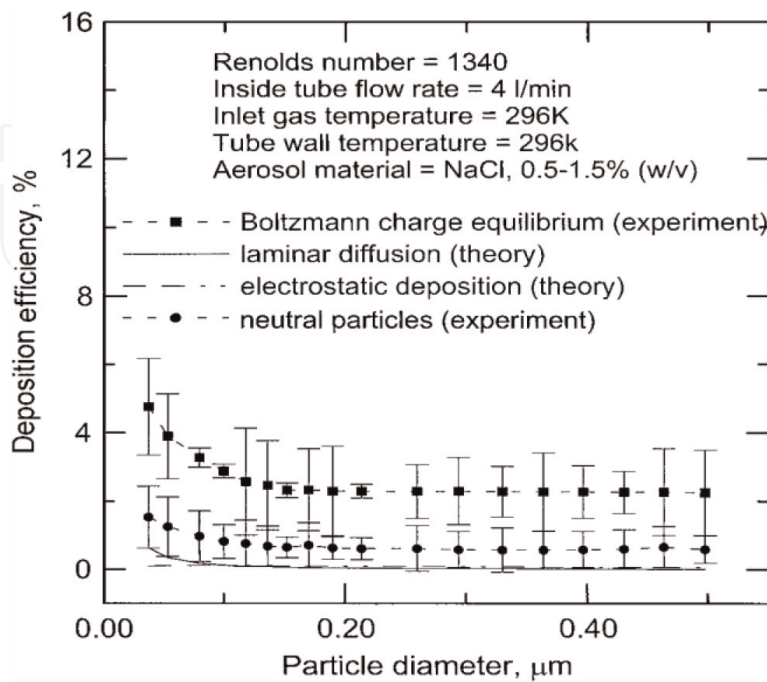


Figure 6. Comparison of experimental deposition efficiencies (nonthermophoretic) and theoretical predictions of diffusional and electrostatic deposition under laminar flow conditions ($Re = 1340$).

The Lee's team studied the effect of thermophoresis on the deposition rate of particles above the wafer in a clean room environment [29, 30]. Using the statistical Lagrangian particle tracking (SLPT) model, under the condition of parallel airflow, particle deposition rates above individual wafers were measured. The law of particle deposition velocity as a function of temperature difference (temperature difference between plane and ambient air), particle density, and parallel airflow velocity is summarized. With and without thermophoresis, some numerical simulation results are as follows. The results show that with the increase of particle density, the particle deposition velocity decreases sharply with the increase of particle size, and the increase of airflow velocity also leads to the increase of particle deposition velocity (Figures 7 and 8).

Research on the deposition effect of particles in pipes or tiny spaces is a very popular direction in thermophoretic research both at home and abroad. Many scholars choose different parameters or channel and space conditions to establish corresponding particle motion models under thermophoretic effects. Yu et al. [31] carried out numerical simulation and analysis on the influence of thermophoretic force in MOCVD horizontal reactor on the concentration distribution of reaction precursors during deposition. For the TMGa molecules in the MOCVD reactor, the calculation formulas of the thermophoretic force, thermophoretic velocity, and diffusion velocity were deduced; Ho et al. [32] studied the effect of thermophoresis on particle deposition rate in mixed convection on vertically corrugated plates, using a cubic spline method, combining dimensionless variables, Prandtl transforms, and parabolic transform to obtain the final result. The results show that the smaller the particle size, the greater the influence of electrophoresis and thermal swimming, the greater the influence of temperature gradient and electric field on the deposition rate of particles.

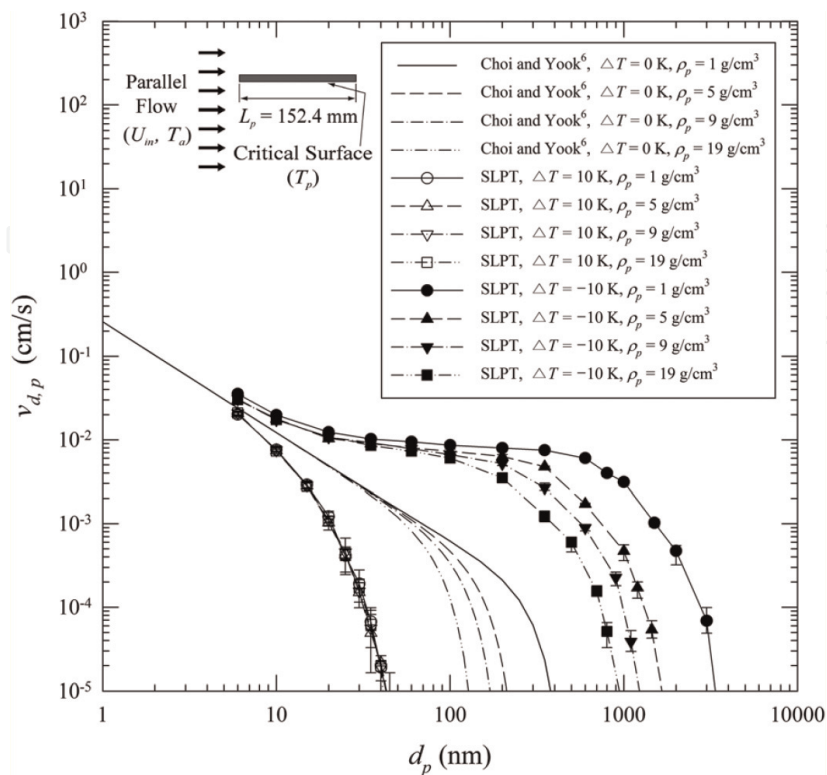


Figure 7.
Effect of particle density.

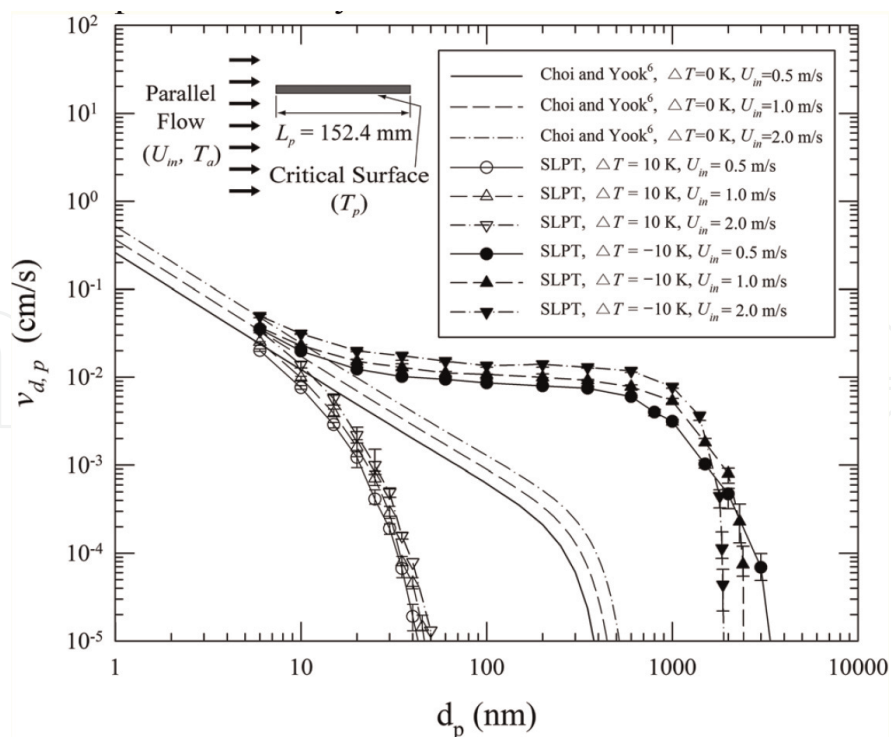


Figure 8.
 Effect of airflow velocity.

3.2 Research on thermophoretic deposition under indoor and outdoor temperature fields

Compared with the first type of work, there are few international studies on particle thermophoretic deposition in indoor temperature fields, and the experimental conditions chosen by various scholars are quite different.

The team of Xu and Chen [33, 34] proposed a zero-equation model to simulate the three-dimensional distribution of indoor air velocity, temperature, and pollutant concentration. This method assumes that turbulent viscosity is a function of length scale and local average velocity. This new computational model is much faster than the standard model. A two-layer model was then used to predict the flow. The model adopts the single equation model for the near-wall region and the standard model for the outer wall region, which improves the calculation efficiency again. Some scholars have also applied it to the utilization of water resources.

Lai [35] used two chambers to simulate indoor and outdoor conditions and the crack module to simulate wall cracks to study the effect of thermophoresis on particle penetration cracks. By simulating summer and winter conditions in temperate climate regions, it is found that the penetration ratio of particles from indoor to outdoor in winter conditions is significantly higher than that in summer and isothermal conditions when the particle size is less than $100 \mu\text{m}$. And the effect of temperature on the particle penetration ratio decreases with the increase of particle size.

3.3 Study on the influence of thermophoresis effect on particle deposition between rotating disks

Due to the geometry of the disk, the fluid flow under the action of the rotating disk is widely used in many engineering fields. In the past decade, with the development of

mechanical technology, the effect of thermophoretic deposition on the fluid flow on the rotating disk has gradually become a hot topic.

Khan and Mahmood [36] investigated the effect of thermophoretic deposition on MHD flow of Oldroyd-B nanofluids between radiatively stretched disks. They used the homotopy analysis method to solve the transformed ordinary differential equations, and analyzed the convergence of the obtained series solutions. Through the analysis of the obtained results, it was found that the fluid temperature and the nanoparticle concentration decreased with the increase of the thermophoretic velocity parameter value. But it will increase with the increase of thermophoretic diffusion parameters. Hafeez et al. [37] also studied the thermophoretic deposition of particles in Oldroyd-B fluid between rotating disks, using von Karman similarity variables to convert partial differential equations into dimensionless ordinary differential equations, and with the help of Maple Numerical format (BVP-Midrich technique) to obtain numerical solutions. The results show that the axial thermophoretic velocity of the particles between the discs increases with the increase of the relative thermophoretic coefficient; the slope of the particle concentration growth curve decreases with the increase of the thermophoretic coefficient; the inward axial thermophoretic deposition velocity (Local Stanton number) increases with the increase of the thermophoresis coefficient (**Figure 9**).

Since the transformed ordinary differential equations are coupled and nonlinear, it is difficult to obtain closed-form solutions. Therefore, in recent years, many scholars have adopted the shooting technique and used the Runge-Kutta integral scheme to solve the ordinary differential equations obtained after similarity transformation. M.S. Alam et al. [38] used this method to study the deposition mechanism of micron-sized particles caused by thermophoresis during transient forced convection heat and mass transfer on an impermeable rotating disk with a surface temperature lower than that of the surrounding fluid. Doh and Muthamilselvan [39] studied the effect of a rotating disk in a uniform electromagnetic field on the deposition of thermophoretic particles during unsteady heat and mass transfer in forced convection in a micropolar fluid. Gowda et al. [40] investigated the deposition of thermophoretic particles in a mixed nanofluidic flow suspended by ferrite nanoparticles. For different fluid or particle objects, most scholars have obtained relatively consistent results on the changing trends of related thermophoretic parameters in the thermophoretic deposition between rotating discs.

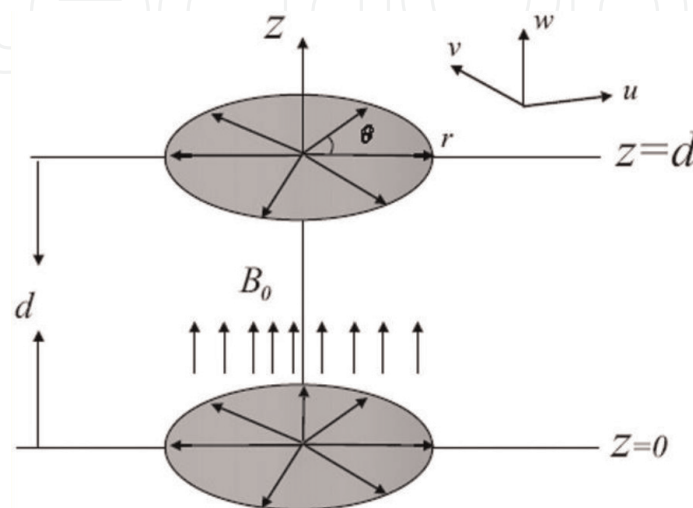


Figure 9.
A physical sketch of the problem by Khan and Mahmood [36].

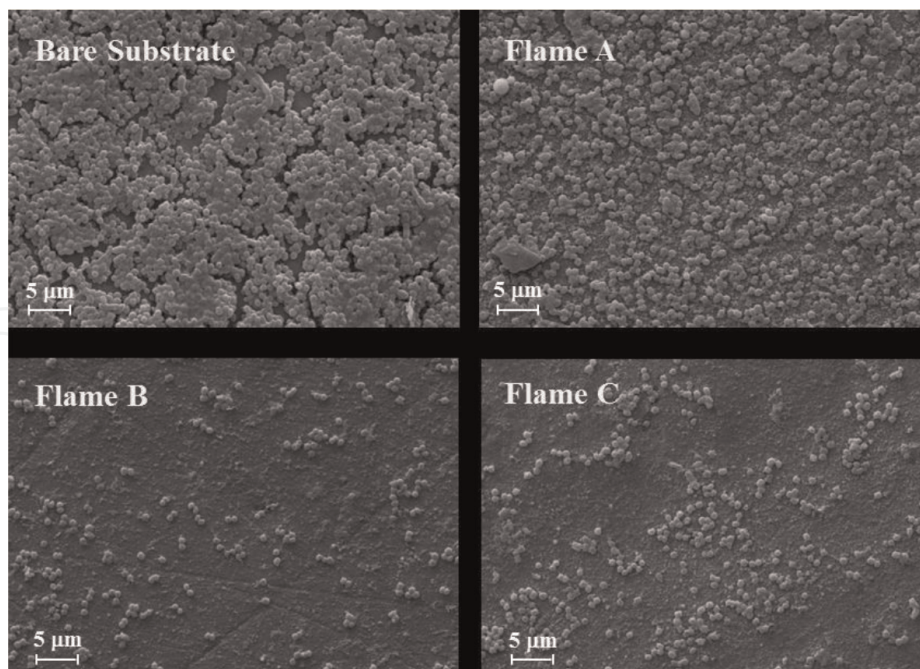


Figure 10.
SEM microphotographs of *Staphylococcus aureus* biofilm on uncoated aluminum substrates and TiO_2 coated aluminum substrates for the three different flame conditions.

3.4 Research on thermophoretic deposition technology in other works

In addition to the above main types of work, thermophoretic deposition technology is also widely used in other aspects. Shi and Zhao [41] considered the deposition velocity of particles on the human body surface under Brownian and turbulent diffusion, gravitational settling and thermophoresis. The results show that for particles below $1\ \mu\text{m}$, thermophoresis is the main deposition mechanism. Brugière and Gensdarmes et al. [42] designed a radial flow thermophoretic velocity analyzer device. By developing the transfer function of the device they designed, the instrument can directly measure the particle velocity in the temperature field with high resolution. Effective thermophoretic velocity, eliminating the need to build a model to calculate the thermophoretic behavior of particles. De Falco et al. [43] achieved a highly controllable and tunable technique for the production of nanostructured TiO_2 coating films on aluminum substrates by combining aerosol flame synthesis and direct thermophoretic deposition. Self-cleaning and self-disinfecting coating materials with near superhydrophilicity and high antibacterial activity can be prepared. As shown, the number of *Staphylococcus aureus* was significantly reduced on the substrate with the titanium dioxide layer (**Figure 10**).

4. Conclusion and outlook

Nowadays, the international research on the thermophoretic deposition effect has been very extensive, and a lot of achievements have been achieved. However, there are still many deficiencies and limitations in both the theoretical understanding of the thermophoretic mechanism and the application of the thermophoretic deposition effect in practical work.

Regarding the understanding of the thermophoretic mechanism, there have been relatively mature research results in the thermophoretic particle motion model in the continuum region and free molecular region, but some scholars have extended their theory to the transition region but found that the results are not ideal; Most of the studies are carried out under the condition that the thermal conductivity of particles is similar to the thermal conductivity of gas. When the thermal conductivity of particles is higher, the experimental results have a large deviation from the theoretical calculation values; In terms of particle shape, there are many studies on spherical particles, and the theoretical and experimental data are in good agreement. However, there are few studies on non-spherical particles, and most of the particles are non-spherical in reality. Errors introduced by thermophoretic force measurements on non-spherical particles may affect the data accuracy of the entire experiment.

In terms of experiments, the experimental conditions selected by various scholars are quite different, and it is difficult to make horizontal comparisons; Thermophoretic force is a short-range force. To obtain higher particle deposition efficiency in practical engineering applications, it is necessary to design an effective removal device structure; In the process of particle deposition, there is often the problem of particle resuspension, so the subsequent treatment of the deposited particles is also very important. At present, many studies have not considered the effects of particle agglomeration and fragmentation. In practical engineering applications, the characteristics of the flow field where the particles are located are usually much more complicated than the conditions selected in the experiment, so there are still many problems to be explored to widely apply thermophoresis technology to practical work.

Acknowledgements

The authors thank the Key R & D plan of Zhejiang Province (2019C03097), National Natural Science Foundation of China (11872353) and Natural Science Foundation of China of Zhejiang Province (LZ22A020004) for their support.

Nomenclature

T	gas temperature
F_T	thermophoretic force
d_p	particle diameter
k_g	fluid thermal conductivity coefficient
k_p	particle thermal conductivity coefficient
T_o	average temperature of fluid near particle
Kn	Knudsen number
k_B	Boltzmann constant
m_g	gas molecular mass
R	particle radius
d_m	equivalent diameter of the channel
C_v	constant volume-specific heat capacity
S_n	conventional momentum adjustment coefficient
S_t	tangential momentum adjustment coefficient
m_p	mass of particles

m_r	reduced mass of gas molecules and particles
$\Omega^{(1,1)*}, \Omega^{(1,2)*}$	dimensionless collision integral, for rigid body collision
C_p	specific heat capacity of gas
T_e	fluid inlet temperatures
T_w	tube wall temperatures
\bar{T}	average temperature
h	convective heat transfer coefficient
L	tube length
D	tube diameter
f	coefficient of friction
u_m	average radial velocity
Pr	Prandtl number of air
K_{th}	thermophoretic coefficient
Q	volume flow

Greek letters

\vec{v}_c	slip velocity of gas
ν	gas kinematic viscosity
μ	fluid viscosity
λ	mean free path of gas molecules
κ	thermal conductivity of gases
ρ	gas density
η_L	thermophoretic deposition efficiency

Abbreviations

FVC	forced vital capacity
PEF	peak expiratory flow
LDV	laser-Doppler velocimeter
SLPT	statistical Lagrangian particle tracking
EDB	electrodynamic balance

IntechOpen

Author details


Yonggang Zhou¹, Mingzhou Yu^{1*} and Zhandong Shi²

1 Laboratory of Aerosol Science and Technology, China Jiliang University, Hangzhou, Zhejiang

2 Zhengzhou Tobacco Research of CNTC, Zhengzhou, China

*Address all correspondence to: mzyu@cjlu.edu.cn

IntechOpen

© 2023 The Author(s). Licensee IntechOpen. This chapter is distributed under the terms of the Creative Commons Attribution License (<http://creativecommons.org/licenses/by/3.0>), which permits unrestricted use, distribution, and reproduction in any medium, provided the original work is properly cited. 

References

- [1] Zhao M, Zhou C, Chan T, Tu C, Liu Y, Yu M. Assessment of COVID-19 aerosol transmission in a university campus food environment using a numerical method. *Geoscience Frontiers*. 2022;**2022**:101353
- [2] Ebenstein A, Fan M, Greenstone M, He G, Yin P, Zhou M. Growth, pollution, and life expectancy: China from 1991–2012. *American Economic Review*. 2015; **105**(5):226-231
- [3] Zwozdziak A, Sówka I, Willak-Janc E, Zwozdziak J, Kwiecińska K, Balińska-Miśkiewicz W. Influence of PM1 and PM2.5 on lung function parameters in healthy schoolchildren—A panel study. *Environmental Science and Pollution Research*. 2016;**23**(23): 23892-23901
- [4] Ström H, Sasic S. The role of thermophoresis in trapping of diesel and gasoline particulate matter. *Catalysis Today*. 2012;**188**(1):14-23
- [5] Harish S, Dhanraj RG, Loganathan GB. An efficiency study on water extraction from air using thermophoresis method. *IOP Conference Series: Materials Science and Engineering*. 2019;**574**(1):012003
- [6] Zheng F. Thermophoresis of spherical and non-spherical particles: A review of theories and experiments. *Advances in Colloid and Interface Science*. 2002; **97**(1–3):255-278
- [7] Bakanov SP. Thermophoresis in gases at small knudsen numbers. *Aerosol Science and Technology*. 1991;**15**(2): 77-92
- [8] Kennard EH. Kinetic theory of gases. *International Series in Physics*. 1938; **57**(39):901
- [9] Epstein, Von Paul S.. Zur Theorie Des Radiometers. 1927;**54**(7-8):537-563
- [10] Talbot L. Thermophoresis of particles in a heated boundary layer. *Mechanical Engineering*. 1980;**1980**: 646-655
- [11] Derjaguin BV, Storozhilova AI, Rabinovich YI. Experimental verification of the theory of thermophoresis of aerosol particles. *Journal of Colloid and Interface Science*. 1966;**21**(1):35-58
- [12] Waldmann L. Die Boltzmann-Gleichung Für Gase Aus Spinteilchen. *Zeitschrift Fur Naturforschung - Section A Journal of Physical Sciences*. 1958; **13**(8):609-620
- [13] Brock JR. On the theory of thermal forces acting on aerosol particles. *Journal of Colloid Science*. 1962;**17**(8):768-780
- [14] Brock JR. The thermal force in the transition region. *Journal of Colloid and Interface Science*. 1967;**23**(3): 448-452
- [15] Derjaguin BV, Yalamov Y. Theory of thermophoresis of large aerosol particles. *Journal of Colloid Science*. 1965;**20**(6): 555-570
- [16] Cha CY, McCoy BJ. Thermal force on aerosol particles. *Physics of Fluids*. 1974; **17**(7):1376-1380
- [17] Wood NB. The mass transfer of particles and acid vapor to cooled surfaces. 1981;**76**:6-93
- [18] Li Z, Wang H. Drag force, diffusion coefficient, and electric mobility of small particles. I. Theory applicable to the free-molecule regime. *Physical Review E - Statistical Physics, Plasmas,*

Fluids, and Related Interdisciplinary Topics. 2003a;**68**(6):1-9

[19] Li Z, Wang H. Drag force, diffusion coefficient, and electric mobility of small particles. II. Application. Physical Review E – Statistical Physics, Plasmas, Fluids, and Related Interdisciplinary Topics. 2003b;**68**(6):061206

[20] Cui J, Jun Jie S, Wang J, Xia GD, Li ZG. Thermophoretic force on nanoparticles in free molecule regime. Wuli Xuebao/Acta Physica Sinica. 2021; **70**(5):1-9

[21] Li W, James E. Measurement of the Thermophoretic Force by Electrodynamic Levitation: Microspheres in air 1995;**26**(7): 1063-1083

[22] Byers RL, Calvert S. Particle deposition from turbulent streams by means of thermal force. Industrial & Engineering Chemistry Fundamentals. 1969;**8**(4):646-655

[23] Batchelor GK, Shen C. Thermophoretic deposition of particles in gas flowing over cold surfaces. Journal of Colloid and Interface Science. 1985; **107**(1):21-37

[24] Romay FJ, Takagaki SS, Pui DYH, Liu BYH. Thermophoretic deposition of aerosol particles in turbulent pipe flow. Journal of Aerosol Science. 1998;**29**(8): 943-959

[25] Housiadas C, Drossinos Y. Thermophoretic deposition in tube flow. Aerosol Science and Technology. 2005; **39**(4):304-318

[26] Lin JS, Tsai CJ. Thermophoretic deposition efficiency in a cylindrical tube taking into account developing flow at the entrance region. Journal of Aerosol Science. 2003;**34**(5):569-583

[27] Tsai CJ, Lin JS, Aggarwal SG, Chen DR. Thermophoretic deposition of particles in laminar and turbulent tube flows. Aerosol Science and Technology. 2004;**38**(2):131-139

[28] Lin JS, Tsai CJ, Chang CP. Suppression of particle deposition in tube flow by thermophoresis. Journal of Aerosol Science. 2004;**35**(10):1235-1250

[29] Kim W-K, Lee S-C, Yook S-J. Numerical investigation of Thermophoretic effect on particulate contamination of an inverted flat surface in a parallel airflow. Journal of the Electrochemical Society. 2011;**158**(10): H1010

[30] Woo SH, Lee SC, Yook SJ. Statistical Lagrangian particle tracking approach to investigate the effect of thermophoresis on particle deposition onto a face-up flat surface in a parallel airflow. Journal of Aerosol Science. 2012;**44**:1-10

[31] Yu HQ, Zuo R, Chen JS, Peng XX. Analysis and numerical simulation of precursor concentration distribution on the influence of Thermophoretic force on deposition process in horizontal MOCVD reactor. Rengong Jingti Xuebao/Journal of Synthetic Crystals. 2011;**40**(4):1033-1038

[32] Ho PY, Chen CK, Huang KH. Combined effects of thermophoresis and electrophoresis on particle deposition in mixed convection flow onto a vertical wavy plate. International Communications in Heat and Mass Transfer. 2019;**101**(January):116-121

[33] Chen Q, Weiran X. A zero-equation turbulence model for indoor airflow simulation. Energy and Buildings. 1998; **28**(2):137-144

[34] Xu W, Chen Q. A two-layer turbulence model for simulating indoor

airflow - Part I. Model development. *Energy and Buildings*. 2001;**33**(6): 613-625

[35] Lai ACK. An experimental study of indoor and outdoor concentrations of fine particles through nonisothermal cracks. *Aerosol Science and Technology*. 2013;**47**(9):1009-1016

[36] Khan N, Mahmood T. Thermophoresis particle deposition and internal heat generation on MHD flow of an Oldroyd-B Nanofluid between radiative stretching disks. *Journal of Molecular Liquids*. 2016;**216**: 571-582

[37] Hafeez A, Khan M, Ahmed J. Oldroyd-B fluid flow over a rotating disk subject to sores–dufour effects and thermophoresis particle deposition. *Proceedings of the Institution of Mechanical Engineers, Part C: Journal of Mechanical Engineering Science*. 2021; **235**(13):2408-2415

[38] Alam MS, Chapal Hossain SM, Rahman MM. Transient thermophoretic particle deposition on forced convective heat and mass transfer flow due to a rotating disk. *Ain Shams Engineering Journal*. 2016;**7**(1):441-452

[39] Doh DH, Muthamilselvan M. Thermophoretic particle deposition on magnetohydrodynamic flow of micropolar fluid due to a rotating disk. *International Journal of Mechanical Sciences*. 2017;**130**(April):350-359

[40] Punith Gowda RJ, Naveen Kumar R, Aldalbahi A, Alibek I, Prasannakumara BC, Rahimi-Gorji M, et al. Thermophoretic particle deposition in time-dependent flow of hybrid nanofluid over rotating and vertically upward/ downward moving disk. *Surfaces and Interfaces*. 2021;**22** (October 2020):100864

[41] Shi S, Zhao B. Deposition of indoor airborne particles onto human body surfaces: A modeling analysis and manikin-based experimental study. *Aerosol Science and Technology*. 2013; **47**(12):1363-1373

[42] Brugière E, Gensdarmes F, Ouf FX, Yon J, Coppalle A, Boulaud D. Design and performance of a new device for the study of thermophoresis: The radial flow thermophoretic analyser. *Journal of Aerosol Science*. 2013;**61**:1-12

[43] Falco G, D, Ciardiello R, Commodo M, Del Gaudio P, Minutolo P, Porta A, et al. TiO₂ nanoparticle coatings with advanced antibacterial and hydrophilic properties prepared by flame aerosol synthesis and thermophoretic deposition. *Surface and Coatings Technology*. 2018;**349**:830-837